# Collective Levels in $^{72, 74, 76, 78}$Se†

Rainer M. Lieder*‡ and James E. Draper
*Crocker Nuclear Laboratory, University of California, Davis, California 95616*
(Received 16 January 1970)

The even selenium isotopes $^{72}$Se, $^{74}$Se, $^{76}$Se, and $^{78}$Se have been investigated by means of the Ge($\alpha$, $2n\gamma$)Se and Ge($\alpha$, $4n\gamma$)Se reactions. The $\gamma$ radiation from these nuclei was studied during the irradiation using techniques of in-beam spectroscopy. The energies of the $\gamma$ rays, their relative intensities, their angular distributions, and their time distributions relative to the 2-nsec beam bunch have been measured. Quasirotational ground-state bands were observed up to 10+ for $^{76}$Se, up to 8+ for $^{74}$Se and $^{78}$Se, and up to 6+ for $^{72}$Se. The level energies are compared to a semiempirical formula.

## INTRODUCTION

We have studied the even selenium isotopes $^{72}_{34}$Se, $^{74}$Se, $^{76}$Se, and $^{78}$Se using in-beam spectroscopy methods. The reactions $^{A}$Ge($\alpha$, $2n\gamma$)$^{A+2}$Se and $^{A}$Ge($\alpha$, $4n\gamma$)$^{A}$Se were used to populate levels in the selenium isotopes, and the $\gamma$ radiation from these nuclei was studied during the irradiation.

The level schemes of $^{76}$Se and $^{78}$Se have been investigated by radioactive decay work.[1] These selenium isotopes have also been extensively studied by means of Coulomb excitation.[2-6] A first 2+ state[2-5] as well as a second 2′+ state[3-6] have been observed. All authors agree that the reduced $E2$ transition probabilities $B(E2)$ for the transitions from the first 2+ state to the ground state are larger than the single-particle value. The most recent publication by Stelson and McGowan[2] gives an enhancement by a factor of 51 for $^{76}$Se and 39 for $^{78}$Se. The $B(E2)$ value for the 2′+→2+ transition is larger by about the same factor.[3,6] The $B(M1)$ value for this transition is $10^{-3}$ times the single-particle value, and the $B(E2)$ value for the 2′+-to-ground-state transition has about the single-particle value. These results are typical for collective excitations. Temmer and Heydenburg[5] studied the first 2+ state in $^{74}$Se and found an enhanced $E2$ transition as well. There are no data available for $^{72}$Se.

Lin[7] studied the collective states in $^{76}$Se and $^{78}$Se, employing inelastic scattering of deuterons. He confirmed a 4+ level and a 3− level in both isotopes and found some evidence for a 0+ level. He interpreted the 2′+ state and the 0+ and 4+ states as members of the two-phonon triplet.

In the light of a semiempirical model,[8-10] where the moment of inertia of the nucleus changes with its angular momentum, the 2+ and 4+ states could be interpreted as members of a quasirotational band. We have chosen to use ($\alpha$, $xn\gamma$) reactions to obtain further information about collective levels of Se isotopes because the large orbital angular momentum of the incoming $\alpha$ particle makes it possible to excite high-spin states. Furthermore, in this type of experiment quasirotational states are preferentially populated, as was first shown by Morinaga and Gugelot.[11]

## EXPERIMENTAL SET-UP AND TARGET PREPARATION

The experimental method has already been described briefly.[12] The $\alpha$-particle beam was provided by the Davis 76-in. isochronous cyclotron. The $\gamma$ radiation detected with a Ge(Li) detector was measured in delayed coincidence with the individual $\alpha$-beam bunch.[13,14] In this manner two-parameter experiments were performed measuring the energy of the $\gamma$ rays as well as their time dependence. The Ge(Li) detector was a planar diode of 6-cm$^2$ area and 6-mm depth. It could be rotated about the target to measure angular distributions. A second Ge(Li) detector was used as a monitor.

The analysis of the $\gamma$-ray spectra was performed in two steps. First, the continuum under each peak was determined by fitting a smooth curve through selected points on both sides of each peak. Second, the location and area of each net peak was determined by fitting standard line shapes to the peaks. The standard line shape was composed of a Gaussian curve joined to an exponential tail on the low-energy side of the photo peak.[15] The square of the Gaussian width, and the location of the joining point with respect to the center of the Gaussian were interpolated from radioactive calibration spectra.

To determine photopeak energies and intensities, the energy calibration as well as the efficiency calibration have to be known. For energy calibration, $\gamma$-ray spectra of radioactive sources were taken immediately after each in-beam experiment. All $\gamma$-ray energies are estimated to be accurate to at least ±1 keV. $^{154}$Eu, for which the intensities are reported[16] with an uncertainty of 5%, $^{154}$Eu, was used for the efficiency calibration of the Ge(Li) de-

tector in the experimental geometry. Taking into account the uncertainty introduced by our efficiency calibration data, we assign an over-all uncertainty of ±7% for our efficiency calibration.

The target materials were oxides of the enriched germanium isotopes with mass number $A = 70$, 72, 74, 76. The enrichment was 91% for the $^{70}$Ge target, 91% for the $^{72}$Ge target, 95% for the $^{74}$Ge target, and 74% for the $^{76}$Ge target. The germanium-oxide powder was uniformly distributed on a Mylar strip and bonded to it with a spray lacquer. The target area was 4 by 10 mm, and the thickness was 20 mg/cm$^2$. This is equivalent to 4-MeV loss for 25-MeV $\alpha$ particles and 2-MeV loss for 60-MeV $\alpha$ particles.

## EXPERIMENTAL RESULTS

The selenium isotopes $^{72}$Se, $^{74}$Se, $^{76}$Se, and $^{78}$Se were investigated with $(\alpha, 2n\gamma)$ reactions and $^{72}$Se, $^{74}$Se, and $^{76}$Se with $(\alpha, 4n\gamma)$ reactions. Examples of two-parameter $\gamma$-ray spectra are shown in Figs. 1–4 for $^{78}$Se, $^{76}$Se, $^{74}$Se, and $^{72}$Se produced in $(\alpha, 2n\gamma)$ reactions. The $\alpha$-beam energy was 29.5 MeV. The counting rate is plotted versus $\gamma$-ray energy

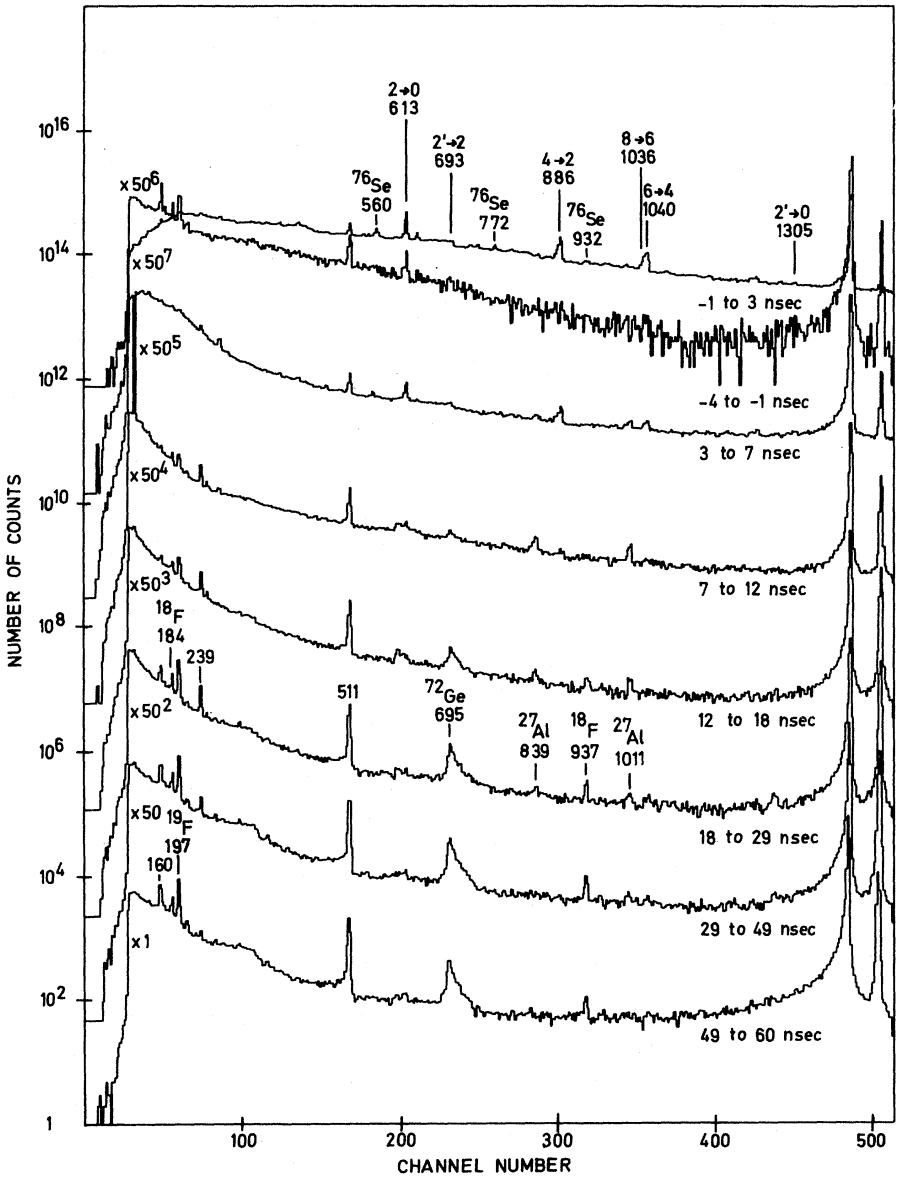


FIG. 1. Two-parameter $\gamma$-ray spectrum for the reaction $^{76}$Ge$(\alpha, 2n\gamma)^{78}$Se. The counting rate is plotted versus pulse height for eight different time bands. The width and location of the time bands is indicated. The beam burst is in the time band labeled −1 to +3 nsec. Energies of the $\gamma$ rays are given in keV. The peaks at the high-energy end of the spectrum are pulser peaks.

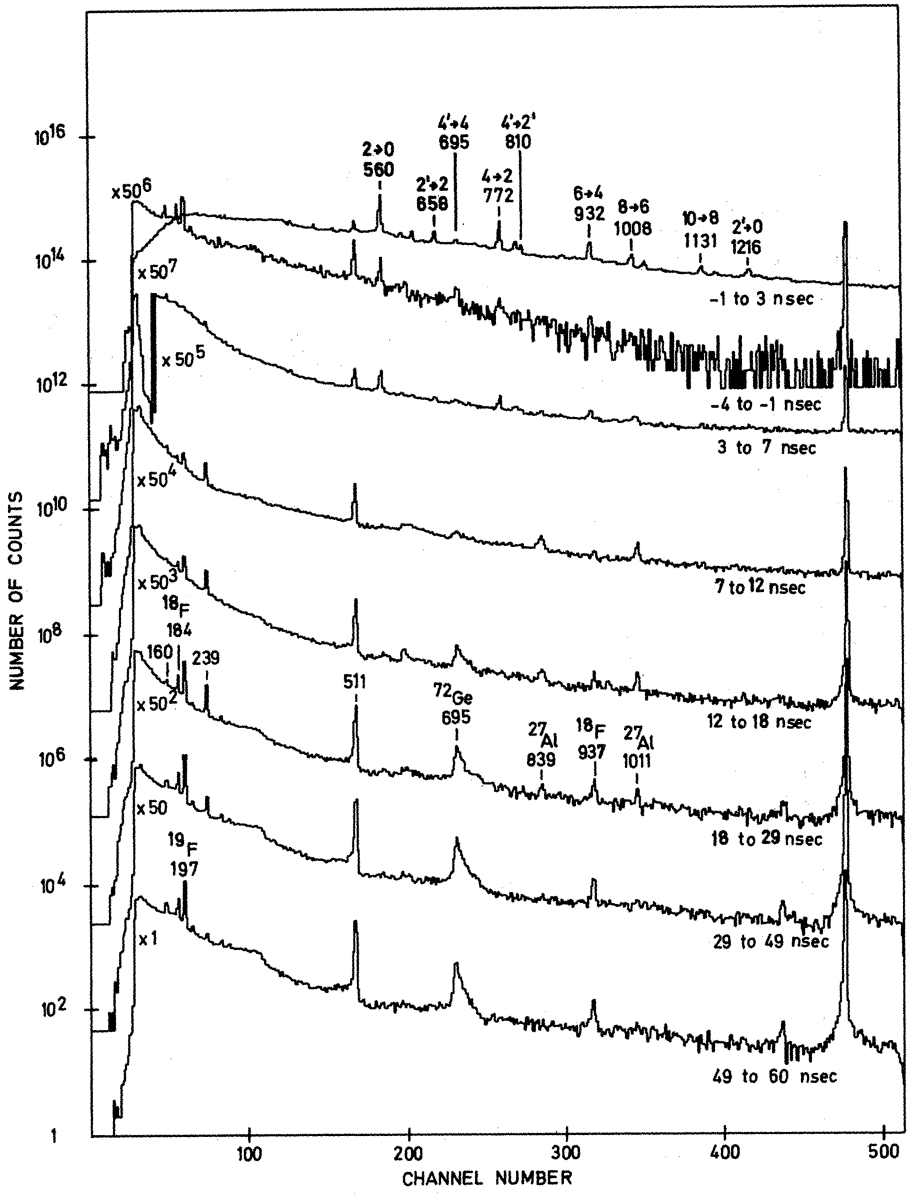


FIG. 2. Two-parameter $\gamma$-ray spectrum for the reaction $^{74}$Ge($\alpha$, $2n\gamma$)$^{76}$Se. For explanations see Fig. 1.

for eight time bands. The width and location of the time bands are indicated.

There are a few lines which are observed in all spectra. They occur in the delayed bands. Most of these are due to the oxygen in the targets, *viz.*, the 184-, 197-, and 937-keV lines or to the aluminum of the apparatus downstream from the target, *viz.* the 839- and 1011-keV lines. The 511-keV peak is due to annihilation radiation, and the uniquely shaped peak at 695-keV is due to the $^{72}$Ge-$(n, n')^{72}$Ge reaction in the detector.[17] The two peaks at the high-energy end of the spectra are pulser peaks. They were used to correct for dead-time losses[12] in the entire electronics system.

The $\gamma$-ray spectrum for the reaction $^{76}$Ge($\alpha$, $2n\gamma$)-$^{78}$Se is shown in Fig. 1. The prompt lines at 613, 693, 886, 1036, 1040, and 1305 keV are assigned as transitions between levels of $^{78}$Se. The 613-, 693-, 886-, and 1305-keV lines have already been assigned as the $2+ \rightarrow 0+$, $2'+ \rightarrow 2+$, $4+ \rightarrow 2+$, and $2+ \rightarrow 0+$ transitions,[1-7] respectively. A few more lines originate from $^{76}$Se produced in the reaction $^{74}$Ge-($\alpha$, $2n\gamma$)$^{76}$Se, since $^{74}$Ge has an abundance of 10% in this target. The other lines are not assigned. The 1036- and 1040-keV lines are not quite resolved although all data clearly indicate a doublet. To resolve these lines a doublet was fitted to the double peak using the shape functions discussed above. This makes the intensities of these two lines *relative to each other* more uncertain than for the other lines investigated.

The $\gamma$-ray spectrum for $^{74}$Ge($\alpha$, $2n\gamma$)$^{76}$Se is shown

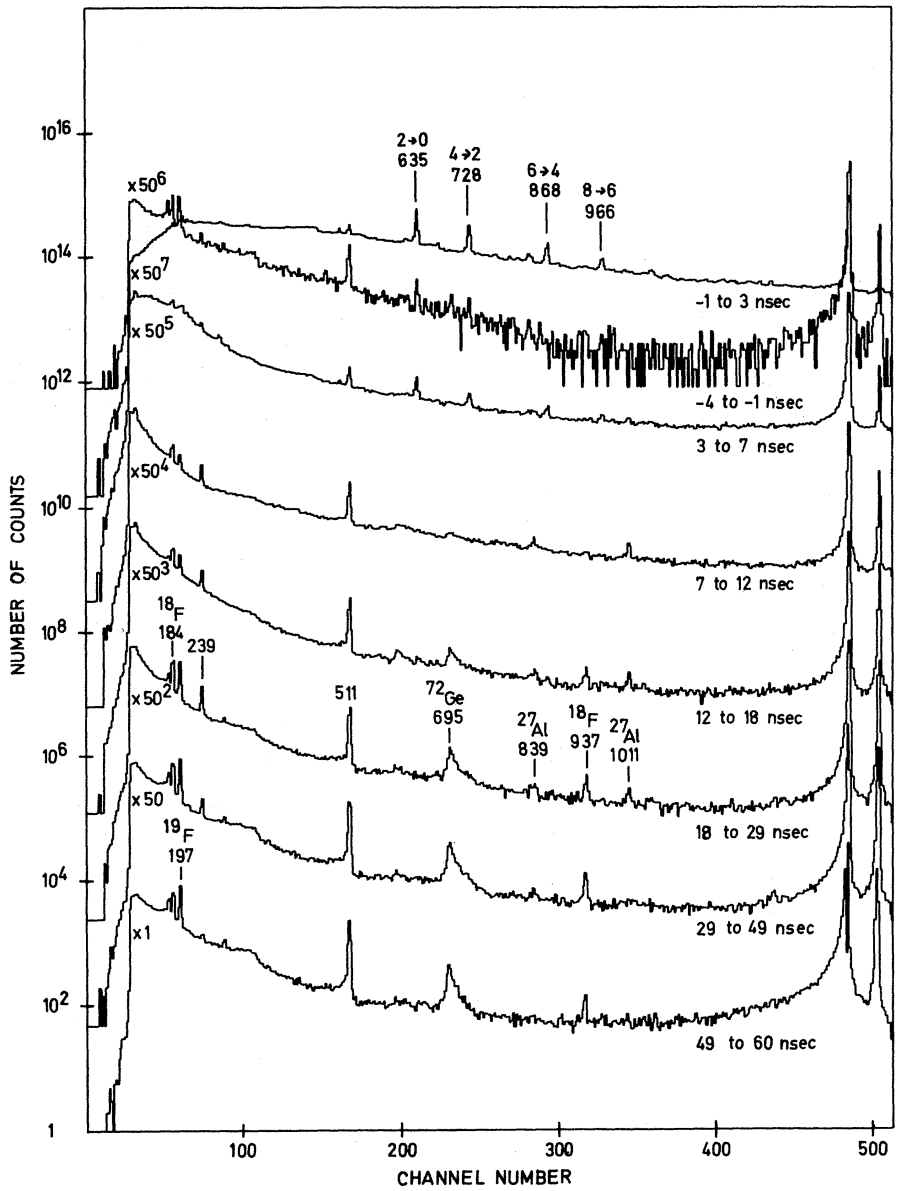


FIG. 3. Two-parameter $\gamma$-ray spectrum for the reaction $^{72}$Ge($\alpha$, $2n\gamma$)$^{74}$Se. For explanations see Fig. 1.

in Fig. 2. The lines at 560, 658, 772, 810, 932, 1008, 1131, and 1216 keV are assigned as transitions in $^{76}$Se. In previous work[1-7] the 560-, 658-, 772-, and 1216-keV lines were assigned as the $2+ \rightarrow 0+$, $2'+ \rightarrow 2+$, $4+ \rightarrow 2+$, and $2'+ \rightarrow 0+$ transitions, respectively.

The $\gamma$-ray spectrum for $^{72}$Ge($\alpha$, $2n\gamma$)$^{74}$Se is shown in Fig. 3. The lines at 635, 728, 868, and 966 keV are assigned as transitions in $^{74}$Se. The 635-keV line was previously assigned[1,5] as the $2+ \rightarrow 0+$ transition in $^{74}$Se.

The $\gamma$-ray spectrum for $^{70}$Ge($\alpha$, $2n\gamma$)$^{72}$Se is shown in Fig. 4. The 775-, 830-, and 862-keV lines are assigned as transitions in $^{72}$Se. None of these lines has been reported before.

To confirm the isotopic assignments of $\gamma$-ray peaks mentioned above, we performed ($\alpha$, $4n\gamma$) reactions on different targets to populate levels in the same isotopes $^{72}$Se, $^{74}$Se, and $^{76}$Se. The isotope $^{78}$Se could not be produced, since $^{78}$Ge is not stable. The $\alpha$ energy was 60 MeV. The $\gamma$-ray spectra for the ($\alpha$, $4n\gamma$) reactions were similar to those obtained with ($\alpha$, $2n\gamma$) reactions. However, the continuum under each peak was higher for the ($\alpha$, $4n\gamma$) reactions, and the weaker lines were obscured. The more intense lines of $^{76}$Se, $^{74}$Se, and $^{72}$Se recurred, however. This, as well as the identification of some lines as previously known transitions, confirmed our isotopic assignment of some of the $\gamma$-ray peaks. The energies and intensities of these

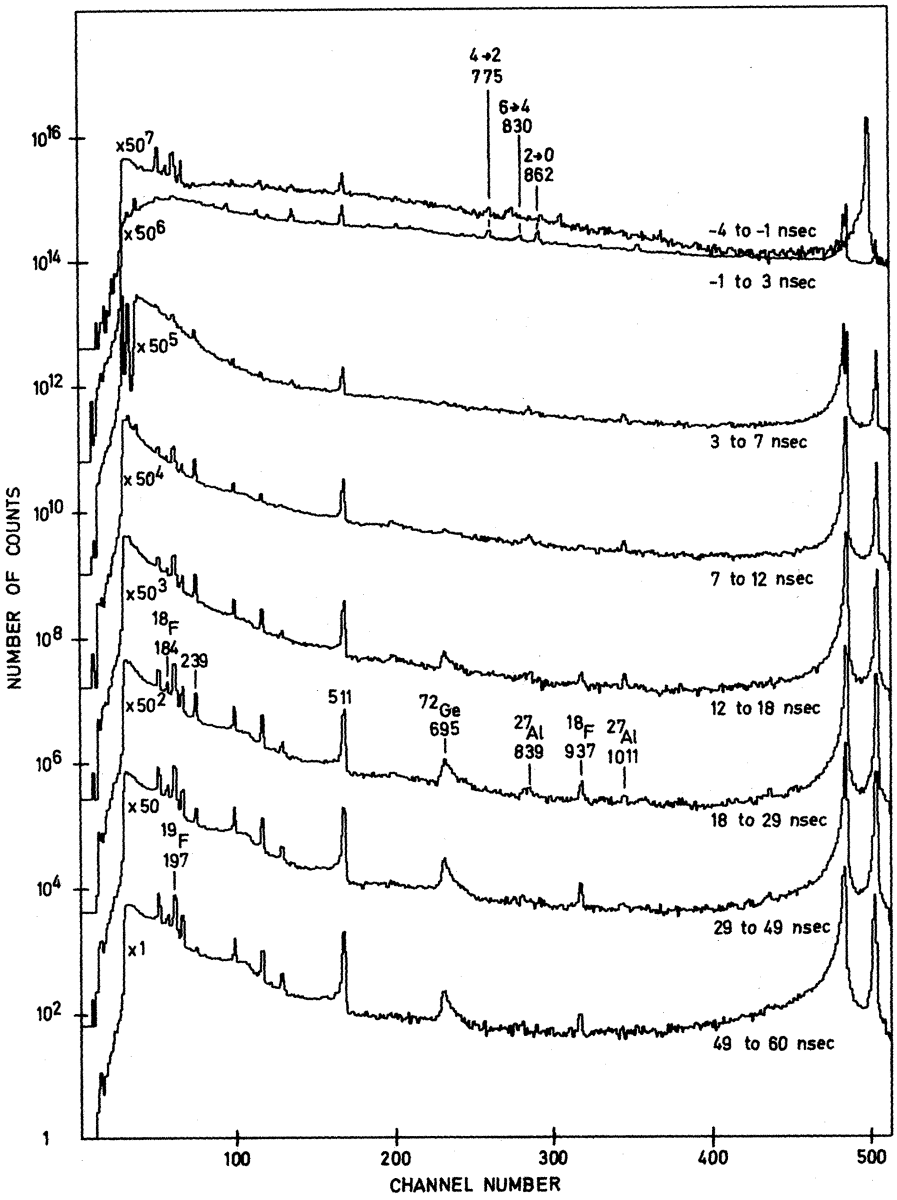


FIG. 4. Two-parameter $\gamma$-ray spectrum for the reaction $^{70}$Ge($\alpha$, $2n\gamma$)$^{72}$Se. For explanations see Fig. 1.

lines are given in the table for $^{78}$Se, $^{76}$Se, $^{74}$Se, and $^{72}$Se. Further confirmation of the isotopic assignments is obtained from the excitation functions, which are discussed later.

The next step is to fit these isotopically assigned transitions into a level scheme. The general approach is discussed in Ref. 12. Most of the lines were found to be $E2$ transitions between quasirotational states, as noted in the table. The data required to support this assignment are the time dependence, the relative excitation functions, and the angular distributions of these $\gamma$ rays as well as systematics of $\gamma$-ray energies and intensities.

The time dependence of the $\gamma$ transitions was measured relative to the $\alpha$-particle beam bunch using the two-parameter spectra as in Figs. 1–4. The distributions for the 2+→0+ transitions in $^{78}$Se, $^{76}$Se, $^{74}$Se, and $^{72}$Se are shown in Fig. 5, in which the counting rate per band divided by the width of the band is plotted versus delay time. The distributions for all the other transitions of interest are similar. All time distributions show a large prompt peak and a small background. This background rate is less than 0.1% the peak rate for the intense 2+→0+ transitions, and less than 1% in all other cases. The prompt peak has a time resolution of 4.0 nsec full width at half maximum and a slope with a half-life of 0.56 nsec on the left side and 0.83 nsec on the right side. This is an upper limit for the half-life of the observed states. This

TABLE I. Experimental results for transitions observed in $(\alpha, 2n)$ reactions at 29.5 MeV.

| Isotope | Energy (keV) | Assignment | Intensity | $A_2$[a] | $A_4$[a] | Multipolarity |
|---|---|---|---|---|---|---|
| $^{78}$Se | 613 | 2+→0+[b] | 1.00 ±0.1 | +0.253 | −0.051 | $E2$ |
| $^{78}$Se | 886 | 4+→2+[b] | 0.78 ±0.08 | +0.283 | −0.061 | $E2$ |
| $^{78}$Se | 1040 | 6+→4+ | 0.44 ±0.06 | +0.317 | −0.077 | $E2$ |
| $^{78}$Se | 1036 | 8+→6+ | 0.23 ±0.03 | +0.332 | −0.086 | $E2$ |
| $^{78}$Se | 693 | 2′+→2+[b] | 0.22 ±0.03 | +0.03 ±0.04 | ··· | $E2$ (+$M1$) |
| $^{78}$Se | 1305 | 2′+→0+[b] | 0.09 ±0.03 | +0.23 ±0.15 | ··· | $E2$ |
| $^{76}$Se | 560 | 2+→0+[b] | 1.00 ±0.1 | +0.245 | −0.049 | $E2$ |
| $^{76}$Se | 772 | 4+→2+[b] | 0.72 ±0.07 | +0.283 | −0.061 | $E2$ |
| $^{76}$Se | 932 | 6+→4+ | 0.40 ±0.04 | +0.316 | −0.077 | $E2$ |
| $^{76}$Se | 1008 | 8+→6+ | 0.22 ±0.03 | +0.333 | −0.087 | $E2$ |
| $^{76}$Se | 1131 | 10+→8+ | 0.11 ±0.03 | +0.337 | −0.090 | $E2$ |
| $^{76}$Se | 658 | 2′+→2+[b] | 0.17 ±0.02 | +0.03 ±0.05 | ··· | $E2$ +2.3% $M1$[c] |
| $^{76}$Se | 1216 | 2′+→0+[b] | 0.14 ±0.03 | +0.14 ±0.09 | ··· | $E2$ |
| $^{76}$Se | 695 | 4′+→4+ | 0.12 ±0.03 | +0.01 ±0.09 | ··· | $E2$ (+$M1$) |
| $^{76}$Se | 810 | 4′+→2′+ | 0.15 ±0.02 | +0.35 ±0.05 | ··· | $E2$ |
| $^{74}$Se | 635 | 2+→0+[b] | 1.00 ±0.1 | +0.292 | −0.070 | $E2$ |
| $^{74}$Se | 728 | 4+→2+ | 0.70 ±0.07 | +0.319 | −0.081 | $E2$ |
| $^{74}$Se | 868 | 6+→4+ | 0.43 ±0.05 | +0.332 | −0.087 | $E2$ |
| $^{74}$Se | 966 | 8+→6+ | 0.24 ±0.03 | +0.336 | −0.089 | $E2$ |
| $^{72}$Se | 862 | 2+→0+ | 1.00 ±0.1 | +0.241 | −0.048 | $E2$ |
| $^{72}$Se | 775 | 4+→2+ | 0.65 ±0.1 | +0.294 | −0.066 | $E2$ |
| $^{72}$Se | 830 | 6+→4+ | 0.42 ±0.1 | +0.316 | −0.076 | $E2$ |

[a] The coefficients of $P_2(\cos\theta)$ and $P_4(\cos\theta)$ for ground-state band transitions are taken from the calculated angular distributions of Figs. 10–13.

[b] Known from previous experiments, see Refs. 1–7.

[c] Multipolarity taken from Grabowski, Gustafsson, and Marklund (Ref. 24).

result supports our assignments, since collective $E2$ transitions are known to be enhanced.

The relative excitation functions were also measured. For $(\alpha, 2n\gamma)$ reactions the $\alpha$-beam energy varied between 25 and 35 MeV, and for $(\alpha, 4n\gamma)$ reactions between 60 and 70 MeV. The intensities of the $\gamma$-ray transitions were normalized to the intensity of the 2+ → 0+ transition for each isotope. The results are shown in Figs. 6–9, where the relative intensity is plotted versus $\alpha$-beam energy for the transitions in the ground-state bands. The error bars of the experimental intensities represent only the statistical uncertainty. The uncertainty introduced by the efficiency calibration is not taken into account, since it does not depend on beam energy.

For all transitions of interest the relative intensity changes slowly with beam energy. This behavior is expected for transitions which belong to the same product nucleus. Only a small increase of the slope of the curves is observed with increasing spin of the initial state. Newton reported[18] a larger increase for the reaction $^{181}$Ta$(\alpha, 2n\gamma)^{183}$Re. We observe about the same relative intensity for $(\alpha, 2n\gamma)$ and $(\alpha, 4n\gamma)$ reactions. The relative intensities for the different transitions help to order the transitions within the band. Because of side feeding of each state from outside the band, the relative intensity of the transitions can only increase for successive transitions in the band.

## ANGULAR DISTRIBUTION MEASUREMENTS

To obtain angular distributions, $\gamma$-ray spectra were taken at the angles 90, 110, 130, and 148° with respect to the direction of the $\alpha$ beam. The $(\alpha, 2n\gamma)$ reactions were used. To normalize the spectra taken at different angles, the output of a pulser triggered by pulses from the monitor detector was also fed into the pulse-height analyzer. The pulser peak contains, therefore, all information[12] about target-source strength, beam fluctuations, and dead-time losses for reasonably prompt transitions.

Large anisotropies have been reported[12,18–21] for the angular distributions of stretched $E2$ transitions within quasirotational ground-state bands. The results of our angular-distribution measurements are shown in Figs. 10–13 for the transitions in the ground-state bands. The anisotropies are large. For each isotope the anisotropy becomes smaller for successive transitions in the ground-state band. This is due to side feeding from out-

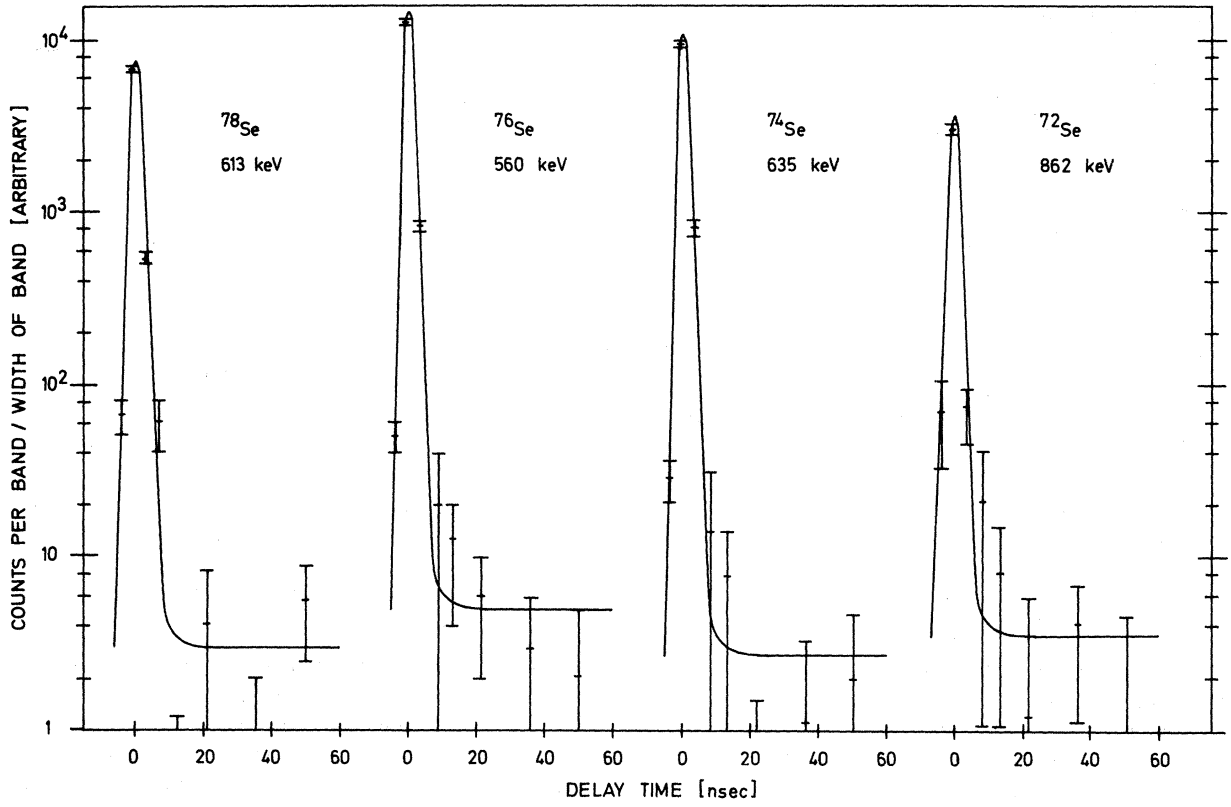


FIG. 5. Time distributions for the 2+ → 0+ transitions in $^{78}$Se, $^{76}$Se, $^{74}$Se, and $^{72}$Se. Plotted is the counting rate per time band divided by the width of the time band versus delay time. The prompt peaks have 4.0 nsec full width at half maximum and slopes with a half-life of 0.56 nsec on the left side and 0.83 nsec on the right side.

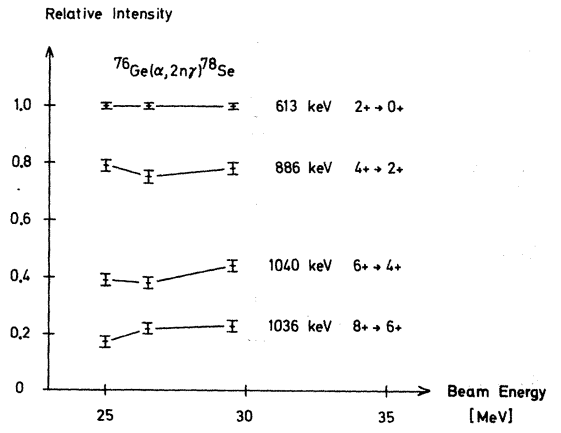


FIG. 6. Relative excitation functions of transitions within the quasirotational ground-state band for the reaction $^{76}$Ge($\alpha$, $2n\gamma$)$^{78}$Se. The intensity of the $\gamma$-ray transitions is normalized to the intensity of the 2+ → 0+ transition. The relative intensity is plotted versus $\alpha$-beam energy.

side the band. For a pure cascade of stretched $E2$ transitions (i.e., no side feeding) the angular distribution is independent of the spins.

The solid curves in Figs. 10–13 are not fits to the data. They are obtained from theoretical calculations in which we assumed[22] that each state in the band is fed by a stretched $E2$ transition from the preceding state as well as by side feeding from outside the band. The angular distributions of these contributions add incoherently. The contribution from cascade feeding has the same angular distribution as the preceding cascade transition. To calculate the angular distribution of the side-feeding branch, it was assumed that side feeding produces a Gaussian distribution of substate population with a width $\sigma$.[22,23] The total angular distribution is obtained as a weighted sum over the contributions from cascade feeding and side feeding. The weights are the experimental transition intensities. The angular-distribution functions in Figs. 10–13 were calculated assuming[22] that the width of the side-feeding Gaussian population distribution depends linearly on the spin $I$ as $\sigma = a + bI$. The parameters $a$ and $b$ were determined by best fit.

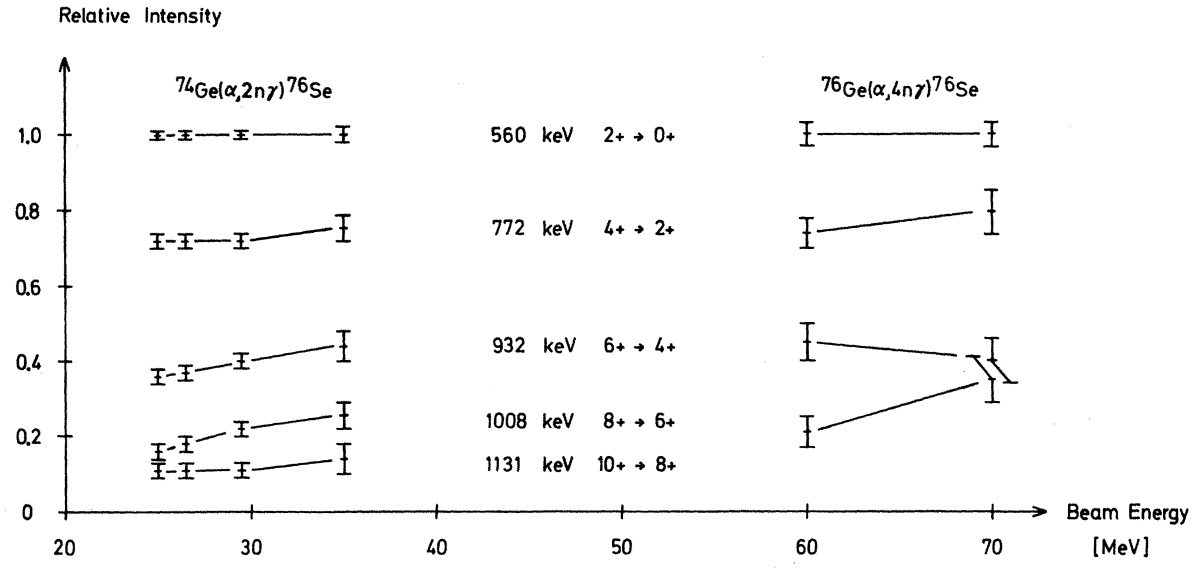


FIG. 7. Relative excitation functions of transitions within the quasirotational ground-state band for the reactions $^{74}$Ge(α, 2nγ)$^{76}$Se and $^{76}$Ge(α, 4nγ)$^{76}$Se.

The calculated results in Figs. 10–13 fit the experimental data well. The rms deviation is in all cases <1.2 times the statistical uncertainty. We used $\sigma = 1.6 + 0.1\,I$ for $^{78}$Se, $^{76}$Se, and $^{72}$Se; and $\sigma = 1.1 + 0.15\,I$ for $^{74}$Se. The uncertainty for $a$ and $b$ is ±0.03.

The experimental angular distributions for the 658-, 695-, 810-, and 1216-keV transitions of $^{76}$Se are shown in Fig. 14. Because of the large statistical uncertainties of these weaker transitions, we fitted only the angular-distribution function $W(\theta) = 1 + A_2 P_2(\cos\theta)$ to the experimental data. The fits are given as solid curves in Fig. 14.

The 1216-keV transition has already been assigned[1-7] as the $2'+ \rightarrow 0+$ transition in $^{76}$Se, making it stretched $E2$. Its angular distribution in Fig. 14 has only a small anisotropy, however, which implies a large $\sigma$ for this $2'+$ state. The 658-keV transition has been assigned as the $2'+ \rightarrow 2+$ transition by Grabowski, Gustafsson, and Marklund,[24]

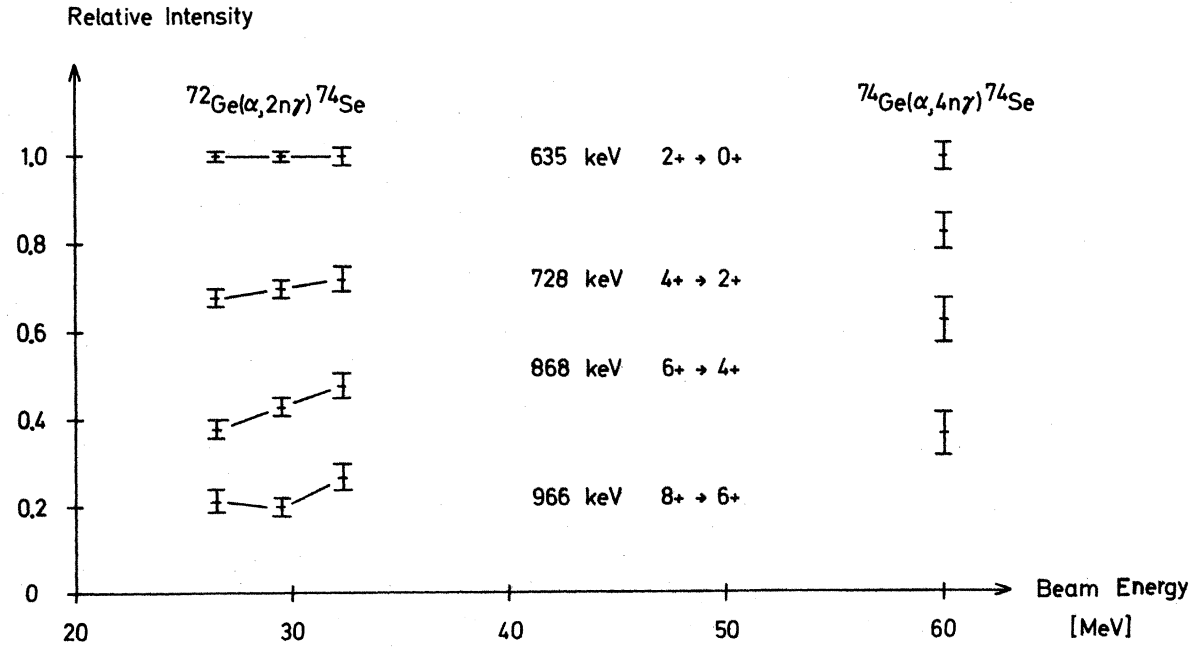


FIG. 8. Relative excitation functions of transitions within the quasirotational ground-state band for the reactions $^{72}$Ge(α, 2nγ)$^{74}$Se and $^{74}$Ge(α, 4nγ)$^{74}$Se.

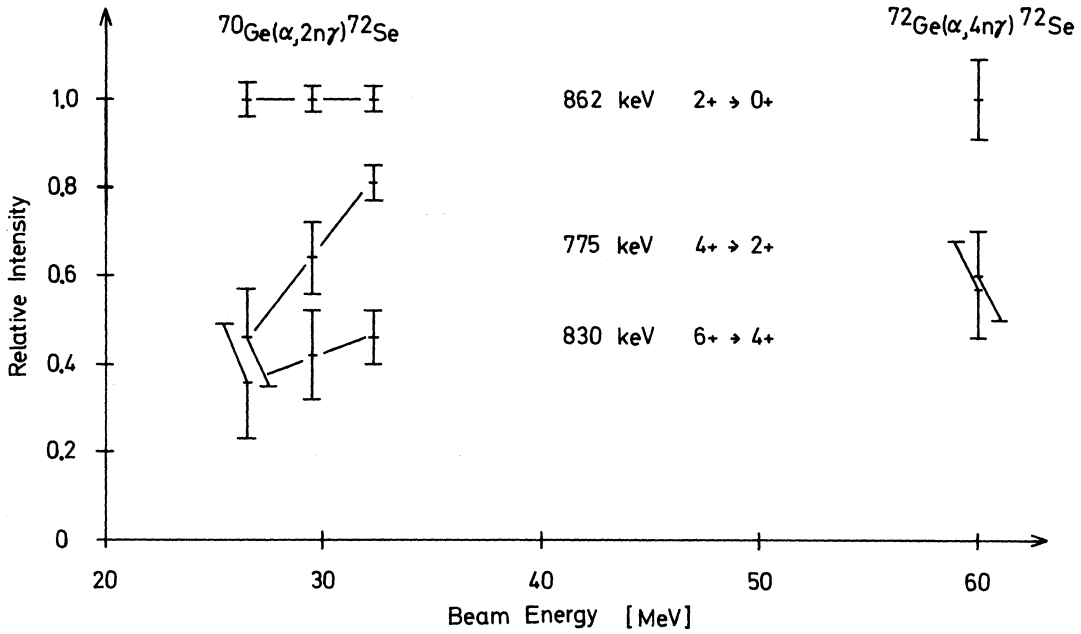


FIG. 9. Relative excitation functions of transitions within the quasirotational ground-state band for the reactions $^{70}$Ge($\alpha$, $2n\gamma$)$^{72}$Se and $^{72}$Ge($\alpha$, $4n\gamma$)$^{72}$Se.

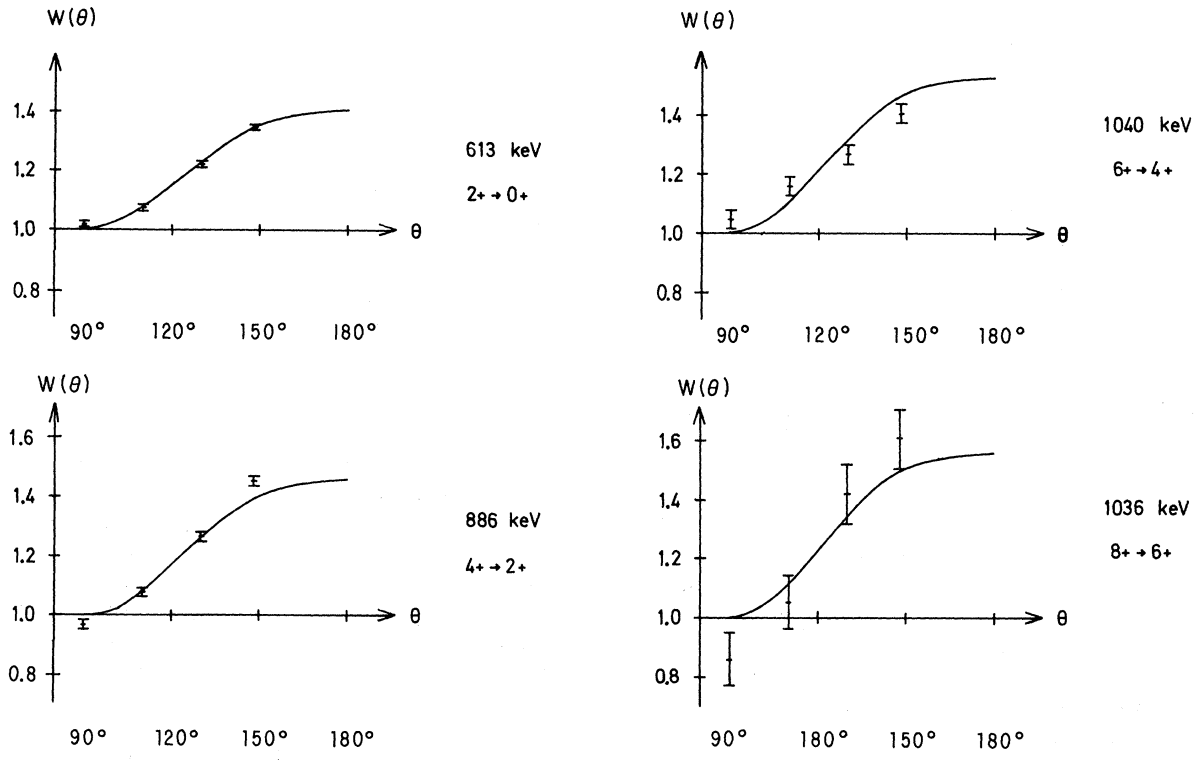


FIG. 10. Angular distributions of transitions with the quasirotational ground-state band for the reaction $^{76}$Ge($\alpha$, $2n\gamma$)$^{78}$Se. The normalized counting rate is plotted versus the angle $\theta$ measured with respect to the direction of the $\alpha$ beam. The solid curves are angular-distribution functions calculated assuming that each quasirotational state of the ground-state band is populated by stretched $E2$ feeding from the preceding rotational state as well as by Gaussian side feeding from outside the band, as discussed in the text.

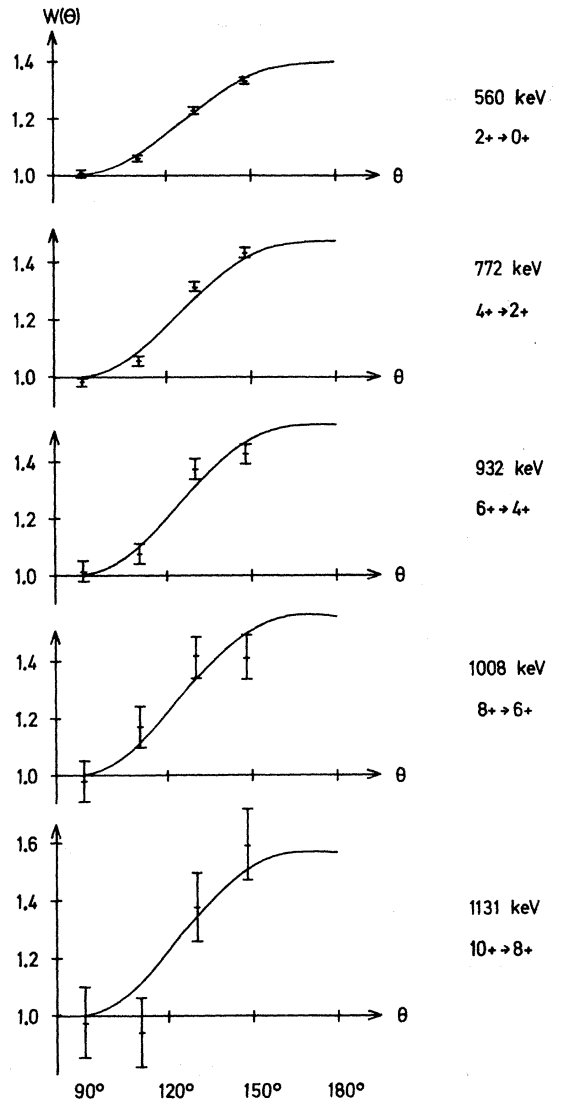


FIG. 11. Angular distributions of transitions within the quasirotational ground-state band for the reaction $^{74}$Ge($\alpha$, $2n\gamma$)$^{76}$Se.

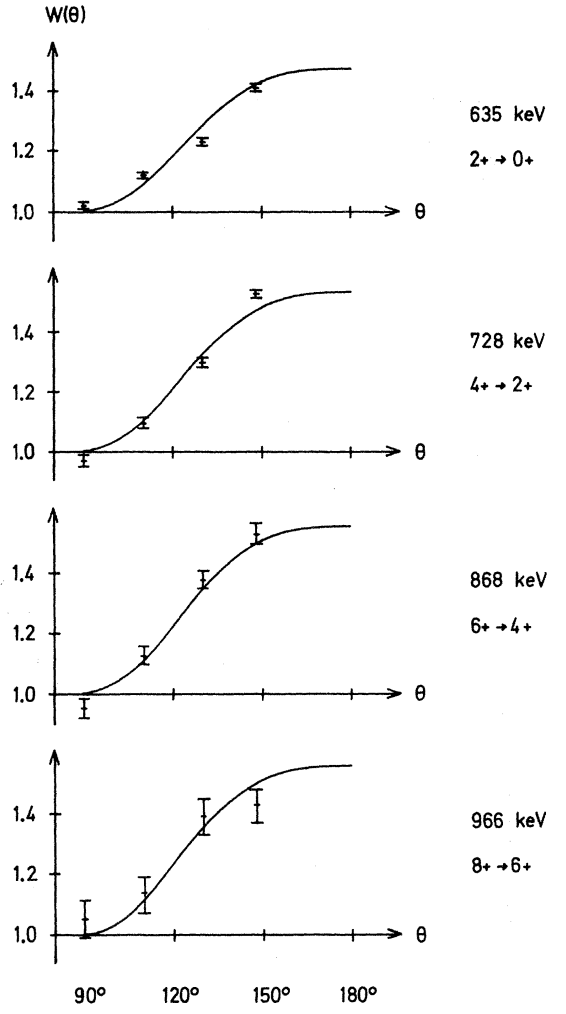


FIG. 12. Angular distributions of transitions within the quasirotational ground-state band for the reaction $^{72}$Ge($\alpha$, $2n\gamma$)$^{74}$Se.

who determined its multipolarity to be $E2 + (2.3 \pm 0.3)\% M1$. Our experimental angular distribution in Fig. 14 is in agreement with this, since a predominantly $E2$ transition between states of the same spin gives an almost isotropic angular distribution for any alignment consistent with the experimental angular distribution of the 1216-keV transition.

The 810- and 695-keV transitions in $^{76}$Se have not been reported before. A calculation of energy sums indicates that these two transitions probably deexcite the same level at 2027 keV. The 810-keV transition populates the 2′+ state, and the 695-keV transition populates the 4+ state. The angular distribution of the 810-keV transition in Fig. 14 has a large anisotropy. This transition, therefore, could be a stretched $E2$ transition from a 4′+ state, or a $M1$ transition from a third 2+ state. The angular distribution of the 695-keV transition, Fig. 14, indicates that this is probably a predominantly $E2$ transition from a 4′+ state. Therefore, we characterize the 2027-keV state as the second excited 4′+ state.

The experimental angular distributions for the 693- and 1305-keV transitions of $^{78}$Se are shown in Fig. 15. The solid curves are again fits of the angular-distribution function $W(\theta) = 1 + A_2 P_2 (\cos\theta)$ to the experimental data. The 1305-keV transition[1-7] is known to be the 2′+→0+ transition. Our experimental angular distribution is in agreement with this interpretation. The 693-keV transition has

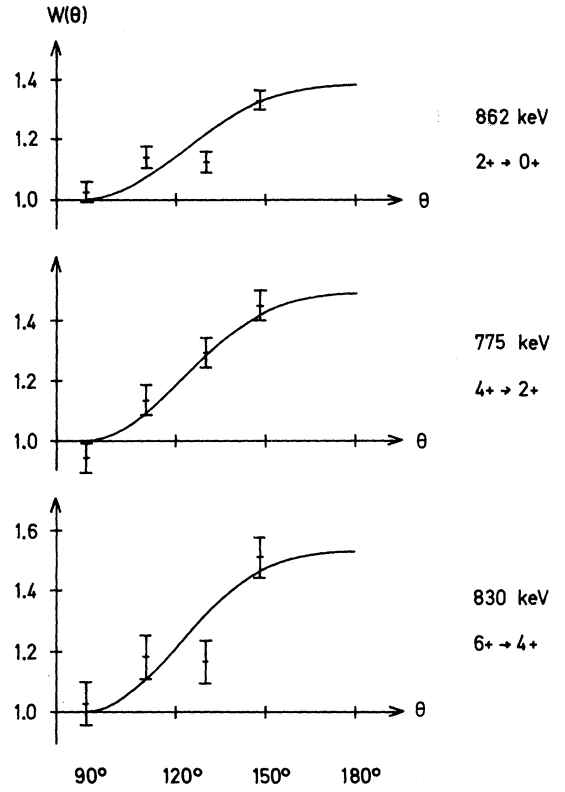


FIG. 13. Angular distributions of transitions within the quasirotational ground-state band for the reaction $^{70}$Ge($\alpha$, $2n\gamma$)$^{72}$Se.

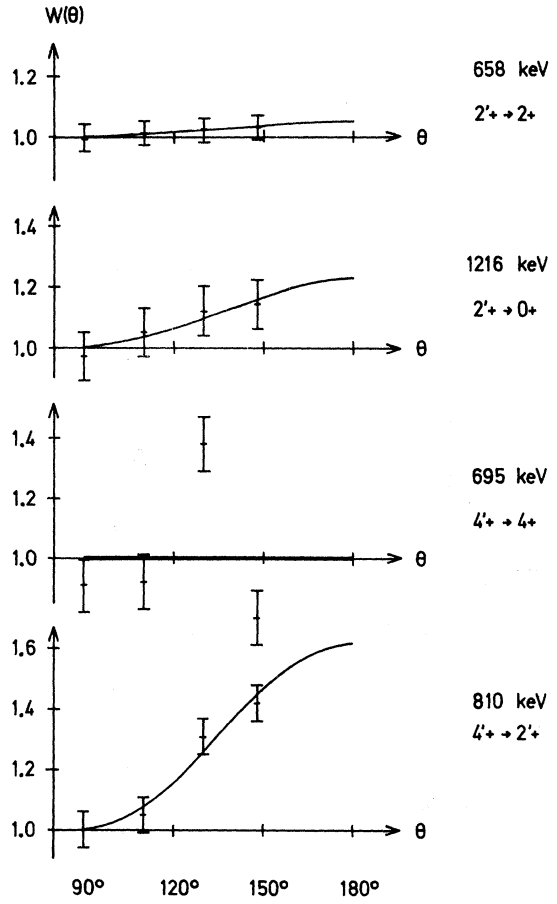


FIG. 14. Angular distributions of transitions outside the ground-state band for the reaction $^{74}$Ge($\alpha$, $2n\gamma$)$^{76}$Se. The normalized counting rate is plotted versus the angle $\theta$ measured with respect to the direction of the $\alpha$ beam. The solid curves are least-squares fits of the function $W(\theta) = 1 + A_2 P_2(\cos\theta)$ to the experimental data.

already been assigned as a $2'+ \rightarrow 2+$ transition.[1-7] The multipolarity is expected[3] to be mainly $E2$. The experimental angular distribution is almost isotropic as required by this assignment, and the alignment consistent with the experimental angular-distribution of the 1305-keV transition.

## DISCUSSION

From these experimental data we propose the level schemes for $^{72}$Se, $^{74}$Se, $^{76}$Se, and $^{78}$Se shown in Fig. 16, which shows levels of the ground-state band up to 10+ for $^{76}$Se, up to 8+ for $^{74}$Se and $^{78}$Se, and up to 6+ for $^{72}$Se. The level of highest spin is observed in the nucleus with the lowest 2+ energy. The level energies vary smoothly with mass number. The relative intensities of each quasirotational transition, normalized to the $2+ \rightarrow 0+$ transition, have about the same values for the different isotopes.

The short lines to the right of each level in Fig. 16 are, to scale, the energies calculated from a semiempirical formula. The origin and tests of this and related formulas are discussed elsewhere.[8-10] The energy $E_I$ of a level of spin $I$ is the

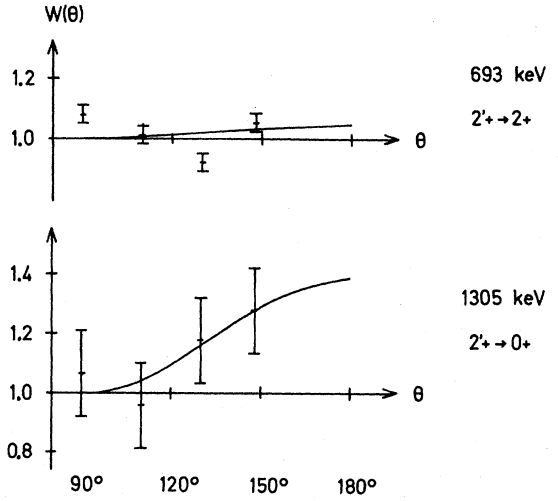


FIG. 15. Angular distributions of transitions outside the ground-state band for the reaction $^{76}$Ge($\alpha$, $2n\gamma$)$^{78}$Se.

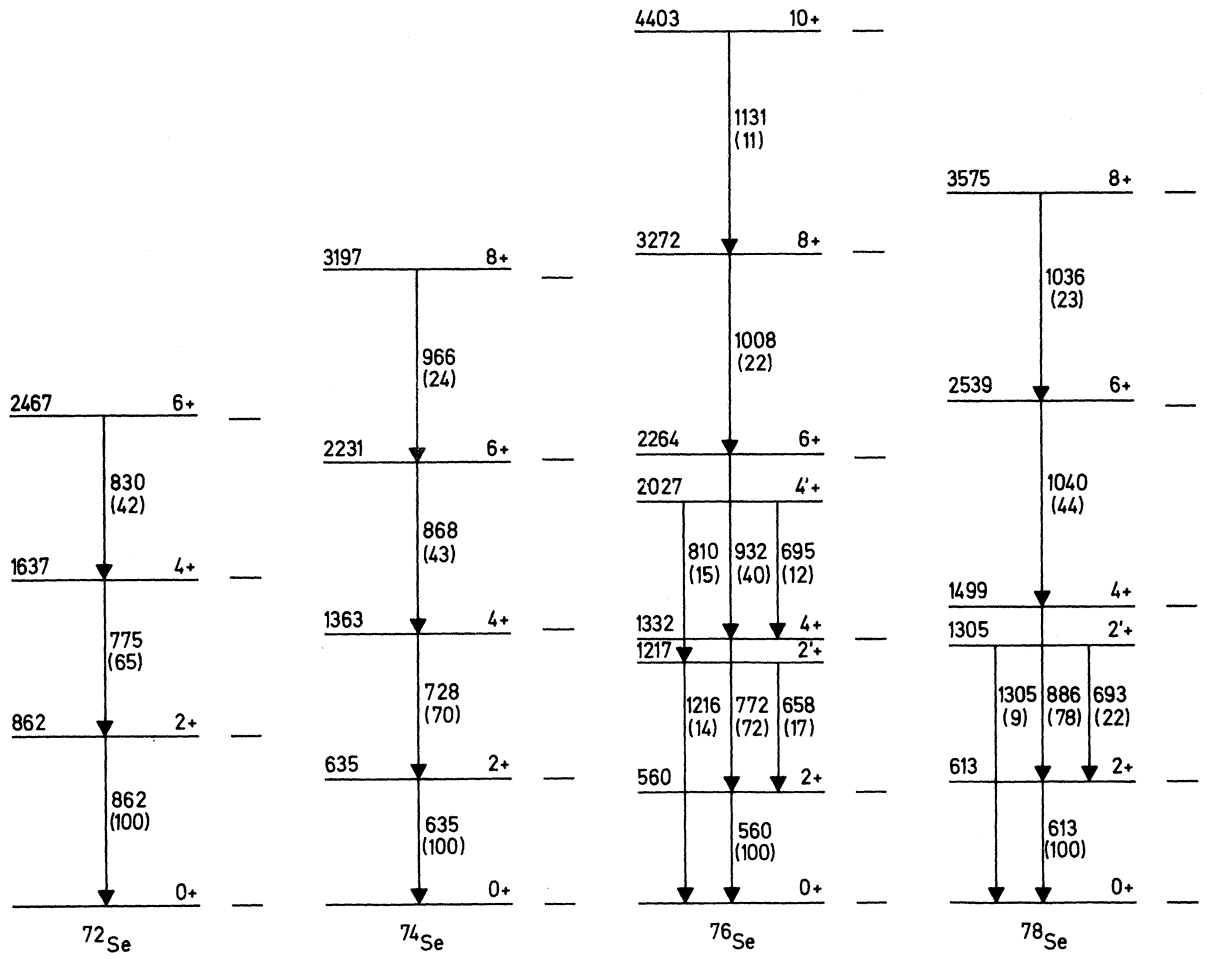


FIG. 16. Level schemes of $^{72}$Se, $^{74}$Se, $^{76}$Se, and $^{78}$Se. Transition and level energies are given in keV. The uncertainties in the transition energies are ±1 keV. Relative intensities are given in parentheses below the transition energy. The level energies obtained by a semiempirical relation are marked as short lines.

minimum of

$$E = \text{const} \times (\delta_I - \delta_0)^2 + \frac{I(I+1)}{2J_I} , \tag{1}$$

with

$$J_I = \delta_I{}^N . \tag{2}$$

The condition of minimization, after substitution of Eq. (2) into Eq. (1), is

$$(\partial E/\partial \delta_I)_I = 0. \tag{3}$$

For the present purpose we regard these as a set of semiempirical equations which give remarkably good fits to experimental energies of quasirotational levels. They were first tested with $N = 1$, 2, 3 by Diamond, Stephens, and Swiatecki[8] for a few nuclei. Later they were tested for $N = 1$ and for $N = 2$ with all available data by Mariscotti,[25] who concluded that if $N$ is to be fixed for all nuclei, the choice of $N = 1$ works better than $N = 2$. The case $N = 1$ was then given by Mariscotti, Scharff-Goldhaber, and Buck.[9] Independently, the case of arbitrary $N$ for each nucleus has been analyzed[10] to determine whether there is a better smooth surface for $N$ than that of $N = 1$.

In order to analyze the present Se results, arbitrary $N$ was used. For the near-optimum choice of $N = 1.2$ for $^{74,76,78}$Se and $N = 1.9$ for $^{72}$Se, the rms deviation of $E_I/E_2$ for all levels in the ground-state bands of Fig. 16 is <1.1% with a maximum error of 1.8%.

The larger value of $N = 1.9$ for $^{72}$Se is primarily caused by the unusual circumstance that $(E_4 - E_2) < E_2$. The ordering of the transitions in $^{72}$Se in Fig. 16 comes entirely from the transition intensities, since there are no other experiments on the levels of $^{72}$Se. This level scheme could only be in error if one of these transitions, e.g., that of 862

keV, is an unresolved doublet of $\gamma$ rays of comparable intensity. That is quite improbable, and there is no experimental evidence of it. If $N = 1.2$ were chosen for $^{72}$Se, as for $^{74,76,78}$Se, then $E_4$ would be 13% too large and $E_6$ would be 19% too large compared with the levels in Fig. 16.

We are indebted to D. G. McCauley, G. L. Smith, R. A. Warner, and W. Wyckoff for their help during the experiments, and to D. G. McCauley for calculating the semiempirical level energies. The kind cooperation of the cyclotron group is gratefully acknowledged. One of us (R.M.L.) wishes to thank the Physics Department and the Crocker Nuclear Laboratory of the University of California, Davis, for their hospitality.

---

†Work partially supported by U. S. Atomic Energy Commission.

*NATO Postdoctoral Research Fellow.

‡Present address: Institut für Kernphysik, Kernforschungsanlage Jülich, 517 Jülich, Germany.

[1]C. M. Lederer, J. M. Hollander, and I. Perlman, *Table of the Isotopes* (John Wiley & Sons, Inc., New York, 1967), 6th ed., and references therein.

[2]P. H. Stelson and F. K. McGowan, Nucl. Phys. 32, 652 (1962).

[3]F. K. McGowan and P. H. Stelson, Phys. Rev. 126, 257 (1962).

[4]D. S. Andreyev, A. P. Grinberg, K. I. Erokhina, and I. Kh. Lemberg, Nucl. Phys. 19, 400 (1960).

[5]G. M. Temmer and N. P. Heydenburg, Phys. Rev. 104, 967 (1956).

[6]Yu. P. Gangrskii and I. Kh. Lemberg, Izv. Akad. Nauk SSSR Ser. Fiz. 26, 1001 (1962) [transl.: Bull. Acad. Sci. USSR, Phys. Ser. 26, 1009 (1962)].

[7]E. K. Lin, Nucl. Phys. 73, 613 (1965).

[8]R. M. Diamond, F. S. Stephens, and W. J. Swiatecki, Phys. Letters 11, 315 (1964).

[9]M. A. J. Mariscotti, G. Scharff-Goldhaber, and B. Buck, Phys. Rev. 178, 1864 (1969).

[10]J. E. Draper, D. G. McCauley, and G. L. Smith, to be published.

[11]H. Morinaga and P. C. Gugelot, Nucl. Phys. 46, 210 (1963).

[12]R. A. Warner and J. E. Draper, Phys. Rev. C 1, 1069 (1970); G. L. Smith and J. E. Draper, Phys. Rev. C 1, 1548 (1970).

[13]R. A. Warner, G. L. Smith, R. M. Lieder, and J. E. Draper, Nucl. Instr. Methods 75, 149 (1969).

[14]T. Yamazaki and G. T. Ewan, Nucl. Instr. Methods 62, 101 (1968).

[15]J. T. Routti and S. G. Prussin, Nucl. Instr. Methods 72, 125 (1969).

[16]G. Aubin, J. Barrette, and S. Monari, Nucl. Instr. Methods 76, 93 (1969).

[17]C. Chasman, K. W. Jones, and R. A. Ristinen, Nucl. Instr. Methods 37, 1 (1965).

[18]J. O. Newton, Nucl. Phys. A108, 353 (1968).

[19]J. O. Newton, F. S. Stephens, R. M. Diamond, K. Kotajima, and E. Matthias, Nucl. Phys. A95, 357 (1967).

[20]D. Ward, R. M. Diamond, and F. S. Stephens, Nucl. Phys. A117, 309 (1968).

[21]T. Yamazaki, G. T. Ewan, and S. G. Prussin, Phys. Rev. Letters 20, 1376 (1968).

[22]J. E. Draper and R. M. Lieder, Nucl. Phys. A141, 211 (1970).

[23]T. Yamazaki, Nucl. Data A3, 1 (1967).

[24]Z. Grabowski, S. Gustafsson, and I. Marklund, Arkiv Fysik 17, 411 (1960).

[25]M. A. J. Mariscotti, Brookhaven National Laboratory Report No. BNL-11838, 1967 (unpublished).